

Chemical modification of a polysaccharide from *Artemisia vulgaris* engenders a supersorbent for the removal of Cd²⁺ from spiked high-hardness groundwater

Muhammad Farid-ul-Haq^a, Arshad Ali^a, Muhammad Ajaz Hussain^{a,*}, Azhar Abbas^a, Fahmeeda Kausar^b, Hatem M.A. Amin^{c,d}, Muhammad Sher^a, Syed Zajif Hussain^e, Irshad Hussain^e

^aInstitute of Chemistry, University of Sargodha, Sargodha 40100, Pakistan, emails: majaz172@yahoo.com (M.A. Hussain), faridulhaq86@yahoo.com (M. Farid-ul-Haq), arshadali04@yahoo.com (A. Ali), azharabbas73@yahoo.com (A. Abbas), msherawan@yahoo.com (M. Sher)

^bSchool of Chemistry and Chemical Engineering (SCCE), Shanghai Jiao Tong University (SJTU), Shanghai, China, email: fchemist32@gmail.com

^cChemistry Department, Faculty of Science, Cairo University, 12613 Giza, Egypt, email: hatem_chem85@yahoo.com

^dChair of Analytical Chemistry II, Faculty of Chemistry and Biochemistry, Ruhr University Bochum, Bochum 44801, Germany

^eDepartment of Chemistry, SBA School of Science and Engineering, Lahore University of Management Sciences, Lahore Cantt. 54792, Pakistan, emails: syed.hussain@lums.edu.pk (S.Z. Hussain), ihussain@lums.edu.pk (I. Hussain)

Received 3 April 2020; Accepted 28 August 2020

ABSTRACT

Development of novel and chemically modified-natural materials for toxic heavy metal ions uptake from aqueous environment is hot topic of research nowadays. Mucilage from the seeds of *Artemisia vulgaris* was chemically modified to succinate then to its sodic form. The materials were characterized by Fourier-transformed infrared, scanning electron microscopy-energy dispersive spectroscopy, and solid-state nuclear magnetic resonance spectroscopy. Batch series of experimentations were carried out to study the effects of sorbent dosage (10–90 mg/50 mL sorbate sample), pH (1–7), the concentration of Cd²⁺ (20–200 mg L⁻¹), contact time (2–90 min), and temperature (298–338 K) on the sorption capacity of the sodic form of a hydrogel. Experimental sorption data were fitted to different isothermal and kinetic models. Langmuir isothermal model and pseudo-second-order kinetic model provided the best fit to the experimental data. Maximum sorption capacities of the sorbent (Q_{\max} in mg g⁻¹) to sorb Cd²⁺ were found to be 263.15 mg g⁻¹ from distilled water and 243.90 mg g⁻¹ from spiked high hardness groundwater. The sorbent was found regenerable. The values of ΔG° , ΔH° , and ΔS° were found negative, which indicated that the sorption process is feasible, spontaneous, and exothermic.

Keywords: *Artemisia vulgaris* hydrogel; Cadmium uptake; Chemisorption; Esterification; Ion-exchange; Regeneration

1. Introduction

The rapid increase in urban growth, industrialization, and human activities engender a large number of pollutants including heavy metals to the water bodies [1].

Heavy metals cause lethal effects on all forms of living organisms even at their small concentrations [2]. Volcanic eruption, mining activities, burning of fossil fuels, refining of crude petroleum, manufacturing of rechargeable Ni-Cd batteries, paint, pigment, and dye manufacturing industries,

* Corresponding author.

and printing and photographic industries are various natural and anthropogenic pathways through which Cd^{2+} are discharged into the environment [3,4]. The maximum recommended concentration of Cd^{2+} in drinking water ranges from 0.003 to 0.005 mg L^{-1} according to WHO (World Health Organization). But the use of Cd^{2+} containing foods leads to the accumulation of Cd^{2+} in the living tissues greater than their permissible limits which cause disorders in body organs. Some of the very appealing and adverse health effects of Cd^{2+} toxicity to humans are pulmonary edema, renal dysfunction, kidney malfunction, bone demineralization, lung insufficiency, renal disturbance, hypertension, and cancer [5,6]. Hence, it is imperative to remove Cd^{2+} from wastewater to make it fit for human consumption.

Several traditional, physical, and chemical methods including coagulation [7], membrane filtration [8], chemical and electrochemical precipitation [9], solvent extraction [10], reverse osmosis and nanofiltration [11], adsorption [12], and ion exchange [13] have been used previously to decontaminate the contaminated waters. Among these methods, physical methods and many chemical methods are less effective and non-selective. The removal of heavy metal ions followed by ion-exchange is predominantly attracting scientific attention nowadays because it is highly efficient and selective [14,15].

Biomaterials being easily available, economical, and environment-friendly attracted the vigil eye of researchers for the removal of Cd^{2+} from aqueous environment. But these bio-sorbents have low sorption capacities and are non-selective [16]. Chemical modification of these biomaterials may improve their efficiency and selectivity for removal of Cd^{2+} from polluted water due to the incorporation of specific functionalities. Over the last two decades, various modification strategies have been practiced for the fabrication of economical and more efficient sorbents. Esterification using succinic anhydride as the esterifying agent is one of the common modification strategies [17]. Sodium salts of these succinylated polysaccharides have gained more consideration for the uptakes of metal ions because of their non-toxic and eco-friendly nature. Moreover, these sodic forms have well-defined functional groups, and natural cross-linking in their polymer backbone makes them water-insoluble thereby facilitating their use in wastewater treatment procedures [18]. Amongst the naturally occurring polysaccharides, polysaccharides obtained from the mucilage of plant seeds, that is, mucilage from the seeds of *Mimosa pudica* [19] and Basil [20] were found to be very effective and material of great choice for Cd^{2+} uptake after their succinylation. The mucilage from seeds of *Artemisia vulgaris* (AVH) consists of anhydroglucose units containing 3 hydroxyls that are feasible to be converted to its potential derivatives with terminal COOH groups. Such groups are advantageous to be converted to their sodic forms to engenders supersorbent for heavy metal ion uptake from solution. This is a novel material and more advantageous than many commercially available materials because of its easy availability, cost effectiveness, modifiable nature, and regeneration over several cycles. Another potential aspect is that such materials can bears single kind of functionalities which might offer selectivity toward metal uptake [21].

Herein, mucilage from seeds of AVH has been converted into AVH-succinate (SAVH) followed by its conversion into sodium salt of SAVH (SSAVH). This SSAVH has then been used for Cd^{2+} uptake from distilled water (DW) and high hardness groundwater (HGW). AVH, SAVH, and SSAVH have been characterized by using different spectroscopic techniques. The influence of various operational parameters such as sorbent dosage, pH, initial metal ions concentration, and temperature on sorption has been evaluated. The experimental data have been fitted to various isothermal and kinetic models to establish a mechanism for this sorption process. Moreover, different thermodynamic parameters, such as a change in free energy (ΔG°), enthalpy (ΔH°), and change in entropy (ΔS°) have been estimated to assess the feasibility of the sorption process. Furthermore, re-generability studies of the novel sorbent SSAVH have also been explored.

2. Materials and methods

2.1. Materials

Seeds of *A. vulgaris* (AV) were obtained from the indigenous marketplace of district Sargodha, Pakistan. Reagents and chemicals used were of analytical grade. Succinic anhydride was provided by Alfa Aesar, Kandel Germany. *N,N*-Dimethylacetamide (DMAc), 4-dimethylaminopyridine (DMAP), $\text{Cd}(\text{NO}_3)_2$, NaHCO_3 , HCl, NaOH, NaCl, ethanol, methanol, and *n*-hexane were provided by Sigma-Aldrich, USA. Samples of high-hardness groundwater (HGW) were collected from different areas of district Sargodha, Pakistan. Some preliminary water analysis of HGW, that is, pH (7.80), Ca^{2+} hardness (224 mg L^{-1}), Mg^{2+} hardness (384 mg L^{-1}), total hardness (2,140 mg L^{-1}), total alkalinity (420 mg L^{-1}), chlorides (4,468 mg L^{-1}), sulfates (1,160 mg L^{-1}), nitrates (6.4 mg L^{-1}), carbonates (420 mg L^{-1}), and bicarbonates (420 mg L^{-1}) was provided by Water Quality Laboratory affiliated with Ministry of Science and Technology, Sargodha, Pakistan. All glassware used during the study was washed and rinsed with acid (HNO_3) before drying in a vacuum oven.

2.2. Isolation of *A. vulgaris* seed mucilage

Seeds of *A. vulgaris* (AV) were cleaned manually and soaked in deionized (reverse osmosis, RO) water for 24 h at room temperature. Nylon mesh was used to separate the extruded mucilage from seeds. The extracted mucilage (AVH) was then washed with *n*-hexane (three times) to remove fat and wax. This AVH was then dried in an oven at 323 K. Finally, dried AVH was ground to a fine powder and stored in an airtight container.

2.3. Synthesis of AVH succinate and its sodium salt

AVH succinate (SAVH) was synthesized by esterifying AVH with succinic anhydride by a previously reported method [22] with a little modification. Briefly, 1.0 g of AVH was stirred in DMAc (30 mL) under nitrogen for 1 h at 353 K. Succinic anhydride (3.70 g) and catalyst DMAP (50 mg) were added into this suspension and stirred for 8 h at the same temperature (353 K). The resulting reaction

mixture was then precipitated in ethanol (200 mL) followed by washing with ethanol (thrice to make the product free from succinic acid and unreacted succinic anhydride). The obtained precipitates were then dried in a vacuum desiccator at 333 K overnight and ground to a fine powder. The SAVH was further treated with a saturated aqueous solution of sodium NaHCO_3 for 2 h to prepare sodium salt of SAVH (SSAVH). The as-obtained SSAVH was repeatedly washed with deionized water until the neutral filtrate was obtained. It was then dried and used as a sorbent for the removal of Cd^{2+} from distilled water (DW) and high hard groundwater (HWG).

2.4. Determination of degree of substitution (DS)

To determine DS, SAVH (100 mg) was stirred with 0.02 M NaHCO_3 (100 mL) for 2 h at 298 K. Then a known volume of NaHCO_3 filtrate was titrated against 0.02 M solution of HCl using methyl orange as an indicator. At the endpoint, the volume of HCl required to neutralize NaHCO_3 was determined. This volume of HCl helps for the determination of DS of SAVH using Eqs. (1) and (2):

$$n_{\text{suc}} = V_{\text{NaHCO}_3} \times M_{\text{NaHCO}_3} - V_{\text{HCl}} \times M_{\text{HCl}} \quad (1)$$

$$\text{DS} = \frac{162.14 \times n_{\text{suc}}}{m_{\text{SAVH}} - 100 \times n_{\text{suc}}} \quad (2)$$

where 162.14 is the molar mass of anhydrous glucose unit in g mol^{-1} and 100 is the net increase in the mass of anhydrous glucose unit in g mol^{-1} for each substituted succinate moieties. n_{suc} stands for the number of moles of free carboxylic acid moieties conjugated with SAVH and m_{SAVH} is the mass of SAVH in g; V_{NaHCO_3} is the volume of the mass of NaHCO_3 titrated against V_{HCl} ; M_{HCl} and M_{NaHCO_3} are the molarities of HCl and NaHCO_3 , simultaneously.

2.5. Calculation of yield

Eq. (3) predicts the efficiency of reaction by calculating the theoretical yield of product:

$$\text{Theoretical yield} = m_{\text{SAVH}} + \left[\frac{m_{\text{SAVH}}}{M_{\text{SAVH}}} \times \text{DS} \times M_{\text{suc}} \right] \quad (3)$$

where m_{SAVH} represents the net mass of succinate of polymer used for the reaction. M_w of SAVH, DS, and M_{suc} indicate the mass of repeating units of SAVH, degree of substitution of succinate moiety, and molar mass of succinic acid, respectively.

2.6. Characterization of AVH, SAVH, and SSAVH

2.6.1. Spectroscopic analyses

FTIR spectra of AVH, SAVH, and SSAVH were recorded on the IR Prestige-21 spectrometer (Shimadzu, Japan) in the range from 4,000 to 400 cm^{-1} using KBr pellet disc method. The solid-state spectra of AVH, SAVH, and SSAVH were acquired on CP/MAS ^{13}C -nuclear magnetic resonance (NMR) spectroscopy (Bruker DRX-400) machine at ambient

temperature. The concentration of Cd^{2+} in the supernatant was determined at 228.8 nm (λ_{max} of Cd^{2+}) in the air-acetylene flame using a flame atomic absorption spectrophotometer (FAAS, AA 6300, Shimadzu, Japan).

2.6.2. SEM-EDS analysis

The scanning electron microscopy (SEM; Nova, Nano SEM 450) furnished with a low energy Everhart–Thornley detector (ETD) was used to record SEM images and energy dispersive X-ray (EDX, Oxford) was used to perform energy dispersive spectroscopic analysis (EDS) of AVH, SAVH, and SSAVH before and after Cd^{2+} sorption.

2.6.3. Determination of zero-point charge pH

To determine pH_{ZPC} of SAVH, the pH drift method [23] was used. Accordingly, the sorbent SSAVH (100 mg) was added to NaCl (0.01 M, 20 mL). 0.1 M HNO_3 or 0.1 M NaOH was used to adjust the initial pH (pH_i) value of NaCl solution in the range 1.0–7.0. The whole mixture was stirred for 48 h at 120 rpm and at 298 K. Later, the solution was filtered and the final pH (pH_f) value of the supernatant liquid was noted. This pH_f is plotted against the pH_i . The pH at which the curve intersects the $\text{pH}_i = \text{pH}_f$ line is taken as pH_{ZPC} of the sorbent. At pH_{ZPC} , the surface of the sorbent is neutral, whereas, it becomes negatively and positively charged if the pH of the solution containing ions of heavy metals is greater or less than pH_{ZPC} , respectively [24]. So, it is necessary to find pH_{ZPC} to monitor the behavior of any sorbent for sorption study.

2.7. Batch sorption experimentation

Sorption experiments were carried out to study the effect of various operational parameters. The effect of sorbent dosage (10–90 mg), the effect of pH (1–7), the effect of initial Cd^{2+} metal ion concentration (20–200 mg L^{-1}), the effect of contact (2–90 min), and the effect of temperature (298–338 K) on the sorption capacity of the sorbent SSAVH were investigated to optimize the ideal conditions at which the sorbent can remove the maximum amount of Cd^{2+} from DW and HWG. In each of these experiments, a sample volume of 50 mL was used. For this purpose, the stock solution (1,000 mg L^{-1} , 500 mL) was prepared by dissolving a 1.21 g of $\text{Cd}(\text{NO}_3)_2 \cdot \text{H}_2\text{O}$ in DW and HWG. This stock solution was further diluted using DW and HWG to required concentrations to perform batch sorption experiments. The 0.1 M HCl and 0.1 M NaOH were used to adjust the pH of solutions. The Cd^{2+} ion solutions (100 mL) were taken in Erlenmeyer flasks (250 mL) and an appropriate amount of sorbent was added to them. Flasks were closed using glass stoppers and solutions were shaken using shaking thermostat machine for an appropriate time at 150 rpm. After filtration, the concentration of Cd^{2+} present in the supernatant layer was determined using FAAS. Eqs. (4) and (5) were exercised to determine the amount of Cd^{2+} removed (q_e in mg g^{-1}) by the sorbent.

$$q_e = \frac{C_i - C_e}{m} \times V \quad (4)$$

$$\text{Percentage metal uptake} = \frac{C_i - C_e}{C_i} \times 100 \quad (5)$$

where q_e (mg g^{-1}), C_i (mg L^{-1}), and C_e (mg L^{-1}) symbolize the sorption capacity of Cd^{2+} at equilibrium, initial and equilibrium concentrations of Cd^{2+} , respectively while V (L) is the volume of the solution containing Cd^{2+} and m (g) is the mass of sorbent SSAVH. The sorption experimental data were fitted to various isothermal and kinetic models and the significance of the data was statistically evaluated by applying t -test.

2.8. Isothermal and kinetic modeling

Freundlich, Langmuir, D–R isotherm, and Temkin isothermal models were used for the determination of sorption capacity of the sorbent. Pseudo-first-order, pseudo-second-order, intraparticle diffusion, and Elovich kinetic models were used to further confirm the mechanism of sorption. All of the said models have been further discussed in sections 3.3.6 (Isothermal modeling) and 3.3.7 (Kinetic modeling).

2.9. Determination of thermodynamic parameters

The values of thermodynamic parameters such as a change in free energy (ΔG°), enthalpy (ΔH°), and entropy (ΔS°) help to determine feasibility, spontaneity, and exothermic or endothermic nature of the sorption process. Effect of temperature on Cd^{2+} sorption was used to determine the values of these parameters, using Eqs. (6)–(8):

$$K_c = \frac{C_{\text{ads}}}{C_e} \quad (6)$$

$$\ln K_c = \frac{\Delta S^\circ}{R} - \frac{\Delta H^\circ}{RT} \quad (7)$$

$$\Delta G^\circ = -RT \ln K_c \quad (8)$$

where C_{ads} (mg L^{-1}) indicates the amount of Cd^{2+} sorbed, C_e (mg L^{-1}) is the equilibrium concentration of Cd^{2+} and K_c is the constant for sorption equilibrium.

2.10. Sorption–desorption studies

Regeneration studies of the sorbent were carried out by stirring SSAVH under optimal conditions with DW and HGW containing Cd^{2+} . After filtration, Cd^{2+} in the supernatant was determined by FAAS. The residue of the filtration, that is, sorbent carrying sorbed Cd^{2+} was agitated with brine (saturated solution of NaCl at room temperature, 100 mL) at 298 K for 24 h. All the sorbed Cd^{2+} ions were desorbed and were replaced by Na^+ . The resultant mixture was then filtered and washed thoroughly with deionized water until it gives the negative test with AgNO_3 . The regenerated sorbent was then air-dried and reused for Cd^{2+} uptake. This process was repeated over five cycles.

All the experimentations were carried out in triplicate and mean values were used to present the results.

3. Results and discussion

3.1. Synthesis of AVH succinate and its sodium salt

AVH was treated with succinic anhydride to synthesize its succinate (SAVH). The yield of the reaction was found to be 78.75% with a DS value of 1.2 for succinic acid functionalities as per anhydrous glucose units. The SAVH was further converted to its sodium salt (SSAVH) by treating with a saturated solution of NaHCO_3 . Fig. 1 shows the schematic diagram of newly fabricated SAVH and SSAVH.

3.2. Characterization of AVH, SAVH, and SSAVH

3.2.1. FTIR Characterization of AVH, SAVH, and SSAVH

The FTIR (KBr) spectra of AVH, SAVH, and SSAVH are shown in Fig. 2. The appearance of a prominent peak of carbonyl functionality at 1736 cm^{-1} in the spectra of SAVH and SSAVH elucidate the successful conversion of AVH to SAVH and SAVH to SSAVH. Moreover, the peak at

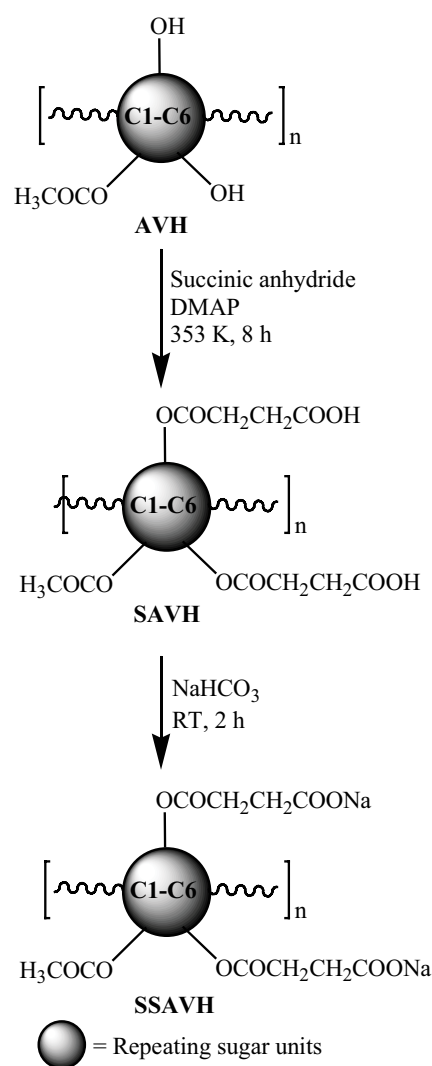


Fig. 1. Schematic diagram for the synthesis of SAVH and its sodic analog SSAVH.

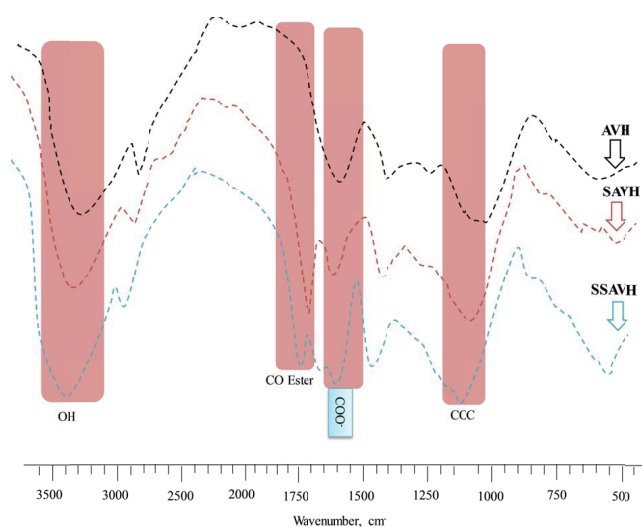


Fig. 2. Cumulative FTIR (KBr) spectrums of AVH, SAVH, and SSAVH.

$1,570\text{ cm}^{-1}$ in the spectrum of SSAVH is due to the presence of carboxylate anion of the sodium salt of SSAVH. Besides these signals, all other fundamental signals representing the polymeric backbone were also present in the spectra of SAVH and SSAVH.

3.2.2. Solid-state CP/MAS ^{13}C NMR spectroscopic analysis

Solid-state CP/MAS ^{13}C NMR spectra of AVH, SAVH, and SSAVH are shown in Figs. 3a–c. These spectra represent the successful conversion of AVH to SAVH and SAVH to SSAVH. In the spectrum of SAVH (Fig. 3b), the appearance of signals at 176.36 ppm represents the presence of ester carbonyl (C7) while signals at 180.41 ppm showed terminal carbonyl group of COOH (C10). Contrary, in the spectrum of SSAVH (Fig. 3c), the carbonyl group of the sodium salt of carboxylic acid (COO^-Na^+) appeared at 184.74 ppm (C10) and ester carbonyl group appeared at 166.88 ppm . Some fruitful information regarding the presence of repeating units of sugar in AVH was also obtained from all spectra. Signals at $21.16\text{--}38.51\text{ ppm}$ are assigned to different CH_2 (C8 and C9) of all succinyl moieties in SAVH. The signals of repeating sugar units appeared at $62.0\text{--}105.15$, $62.23\text{--}105.22$, and $66.90\text{--}104.93$ for AVH, SAVH, and SSAVH, respectively [17].

3.2.3. SEM-EDS analysis

The surface morphology of the products AVH, SAVH, SSAVH, and Cd^{2+} -SAVH was investigated by SEM (Figs. 4e–h). The surface of all these compounds was found to be irregular and unsynchronized. EDS analyses confirmed the presence (Fig. 4d) and displacement of Na^+ ions present in sorbent before and after Cd^{2+} ions sorption, respectively (Figs. 4c–d).

3.2.4. Determination of zero-point charge pH

The zero-point charge pH (pH_{ZPC}) of a sorbent is measured to predict the change in the surface charge of the

sorbent by changing pH. The pH_{ZPC} for SSAV (Fig. 5) was found to be 4.6. The surface of SSAVH will acquire a negative charge at pH greater than 4.6 thereby facilitating metal ion uptake [25].

3.3. Batch sorption experimentation

3.3.1. Effect of pH

The ion exchange affinity of any sorbent depends upon the degree of ionization and surface charge of the sorbent which in turn depends upon the pH of metal ion solution. Fig. 6 shows the effect of pH on the sorption capacity of the sorbent. It was observed that at acidic pH, a negligible amount of Cd^{2+} was sorbed by SSAVH due to protonation of SSAV making the surface of the sorbent positively charged which does not favor the sorption of Cd^{2+} . At pH values greater than pH_{ZPC} (4.6), the surface of the sorbent becomes negatively charged which facilitates the uptake of positively charged Cd^{2+} . Maximum sorption (235.5 mg g^{-1} from DW and 219.33 mg g^{-1} from HGW) was noted at pH 6.0. Furthermore, as the pH of Cd^{2+} solution was increased from 6, then Cd^{2+} precipitated and partially hydrolyzed to $\text{Cd}(\text{OH})_2$. As a result, the concentration of Cd^{2+} ions in the solution decreased and sorption efficiency was suppressed [26,27]. Consequently, pH = 6 was considered as an optimum pH to carry out all other sorption experiments.

3.3.2. Effect of sorbent dosage

To evaluate the minimum amount of sorbent (SSAVH) that can remove the maximum amount of sorbate (Cd^{2+}), the effect of sorbent dosage on the sorption capacity of the sorbent was carried out (Fig. 7a). A sample volume of 50 mL was used. It was observed that by increasing sorbent dose, sorption capacity was increased and found to be highest at 30 mg of sorbent dose. So, 30 mg was chosen as an optimal amount of the sorbent dose. An increase in sorbent dose after 30 mg decreases sorption capacity. This might be attributed to the fact that with the increase in sorbent dose, responsible active sites remain unsaturated, and no more ions are available to be sorbed [20] therefore sorption capacity was decreased after the optimum level.

3.3.3. Effect of initial metal ion concentration

The effect of initial metal ion concentration on the sorption capacity of the sorbent was evaluated and presented in Fig. 7b. Results revealed that with an increase in the Langmuir isothermal model and pseudo-second-order kinetic model provided the best fit to the experimental data and initial concentration of Cd^{2+} , sorption capacity was also increased until it became constant. The reason behind might be, as the concentration of metal ions was increased, more and more ions were exchanged with active sites of the sorbent. After saturation, as all the exchangeable ions of sorbent (Na^+) were exchanged with ions of sorbate (Cd^{2+}), and no more active sites were available for any additional metal ions. Hence, the sorption capacity becomes nearly constant. The 80 mg L^{-1} was found to be an optimum initial metal ion concentration at which SSAV showed maximum sorption capacity.

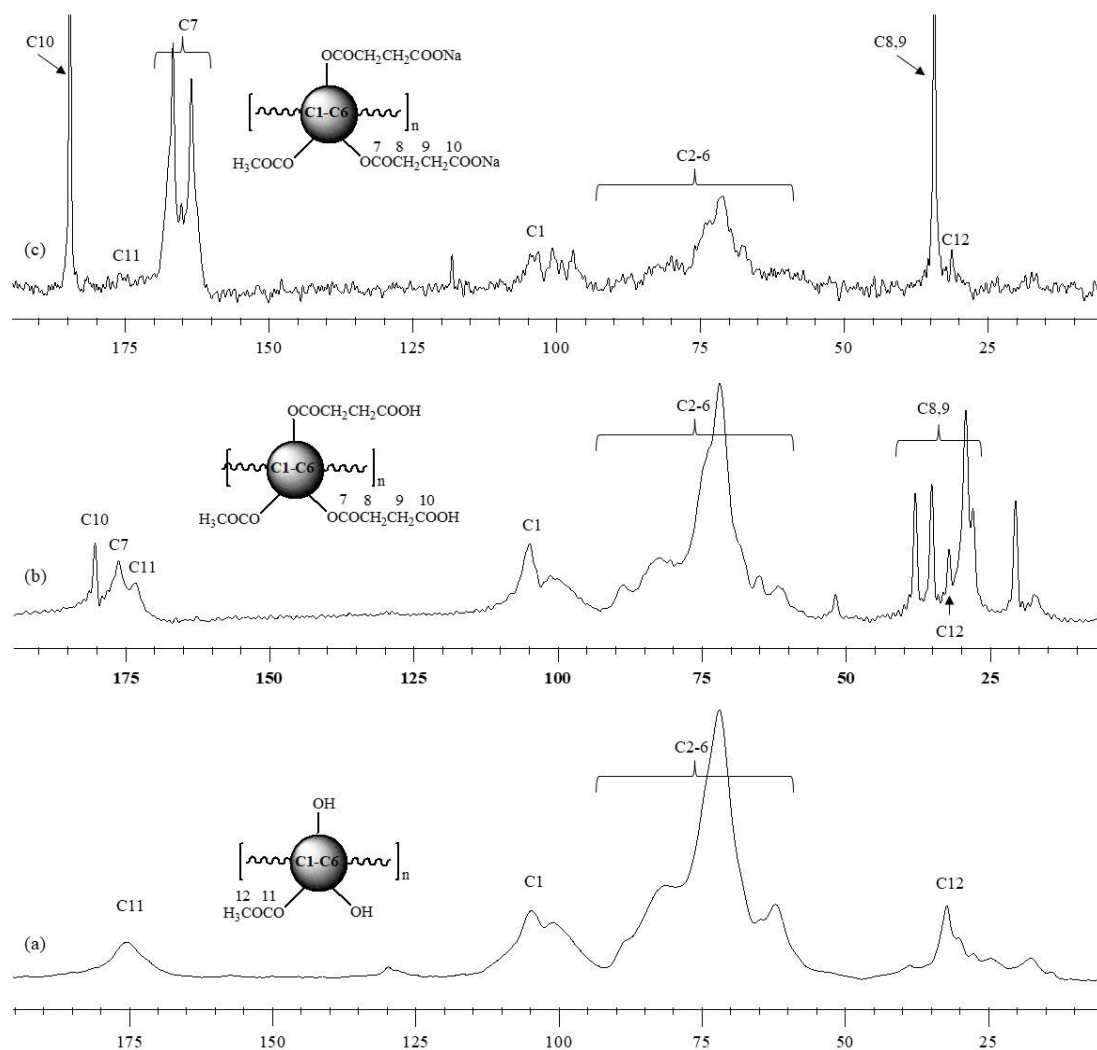


Fig. 3. Solid-state CP/MAS ^{13}C NMR spectrum of AVH (a), SAVH (b), and SSAVH (c).

3.3.4. Effect of interaction time

Fig. 7c shows the effect of contact time on the sorption capacity of sorbent (SSAV). This effect was used to decide about the sorption mechanism and to build kinetic models. Results showed that more than 90% of Cd^{2+} ions were removed from DW and HGW within the first 20 min. It means, 90% of available Na^+ ions on the surface of the sorbent were exchanged with metal ions in solution within this 20 min time. With an increase in contact time beyond 20 min, there were no active sites available on the surface of the sorbent to exchange with metal ions. Hence, no more significant increase in sorption capacity was observed after the optimum time of 20 min.

3.3.5. Effect of temperature

The effect of temperature on the sorption capacity of sorbent was executed to envisage the thermodynamic behavior of the sorption process. The results revealed that with an increase in temperature from 298 to 338 K, a decrease in the sorption capacity of SSAVH for the uptake

Cd^{2+} was observed as shown in Fig. 7d. It is because, at low temperature, the interaction between Cd^{2+} and active site of sorbent was stronger due to less mobility of Cd^{2+} whereas, at high temperature due to kinetic energy and transport of ions, this interaction was weakened.

3.3.6. Isothermal modeling

In sorption studies, sorption equilibrium is one of the fundamental properties to be established to determine the net amount of species adsorbed under the given set of conditions. To optimize the design of a sorption phenomenon for the removal of Cd^{2+} from DW and HGW, it is important to find the most appropriate correlation for the equilibrium curves. In this study, the experimental data obtained from the effect of concentration on the sorption capacity of SSAVH to sorbed Cd^{2+} from DW and HGW was used to establish sorption isotherms viz. Freundlich, Langmuir, Temkin, and Dubinin–Radushkevich isotherm model (D–R) models.

The Freundlich isotherm applies to heterogeneous surface energy systems and it was used to describe the

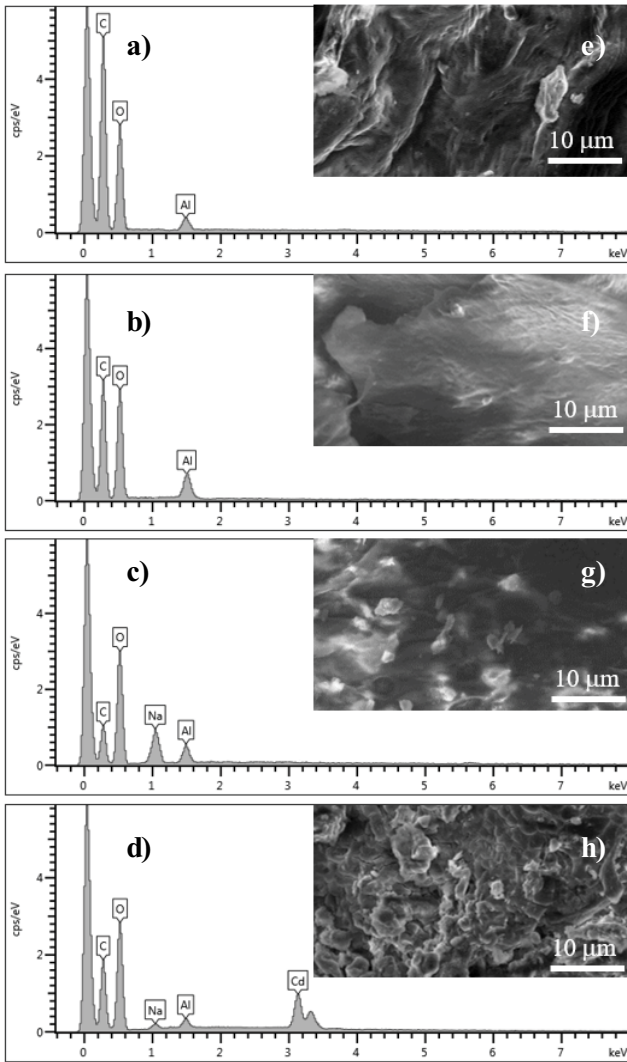


Fig. 4. EDS spectra (a–d), and SEM images (e–h) AVH, SAVH, SSAVH, and Cd²⁺-SAVH.

monolayer or multilayer sorption pattern of sorbent after interaction with sorbate. The linear form of Freundlich isotherm is as:

$$\log q_e = \log K_f + \frac{1}{n} \log C_e \quad (9)$$

In this Eq. (9), C_e (mg L⁻¹) and q_e (mg g⁻¹) are the amounts of metal ions in the liquid phase and metal ion sorbed by sorbent at equilibrium, respectively. K_f (sorption capacity) and n (sorption strength) are the constants associated with this model. To determine the values of these constants and suitability of the model for sorption, the experimental data were fitted by plotting the graph between $\log q_e$ vs. C_e . Slope and intercept of the obtained straight line give the value of n (1.434 for DW and 1.117 for HGW) and K_f (8.043 for DW and 2.294 for HGW), respectively. The enormous deviation of sorption capacity calculated from this isotherm model from experimental values and the very low values of R^2 from DW and HGW shows that

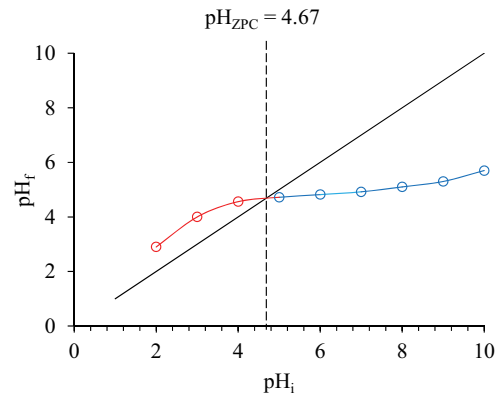


Fig. 5. Zero-point charge pH (pH_{ZPC}) analysis of SSAVH.

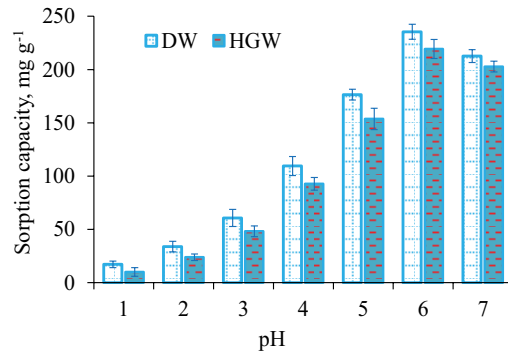


Fig. 6. Effect of pH (1–7) on sorption capacity (q_e in mg g⁻¹) of SSAVH for the removal of Cd²⁺ from DW and HGW (optimum sorption conditions: sorbent dose = 30 mg, pH = 6, Cd²⁺ concentration = 80 mg L⁻¹, contact time = 20 min, and temperature = 298 K in 100 mL solution for both DW and HGW).

this isotherm model did not fit to the experimental data (Fig. 8a, Table 1).

As per the basic principle assumption of Langmuir's theory, the sorption can only occur at specific homogeneous sites inside the sorbent and once a sorbent occupies a site, no more sorption can occur there. So, the data were fitted to this model to describe whether the Cd²⁺ uptake occurs on a homogeneous surface by forming monolayer with or without any interaction between the molecules to be sorbed. Linear form of the Langmuir model is given in Eq. (10):

$$\frac{C_e}{q_e} = \frac{C_e}{Q_{max}} + \frac{C_e}{Q_{max} \times b} \quad (10)$$

In this equation, C_e (mg L⁻¹), q_e (mg g⁻¹), and Q_{max} (mg g⁻¹) are the amount of metal ions in the liquid phase, metal ions sorbed by sorbent at equilibrium and maximum sorption capacity of sorbent, respectively. Whereas, b is the constants associated with this isotherm model. The experimental data were fitted by plotting graph between C_e/q_e vs. C_e and the values of Q_{max} and b were calculated from the slope and intercept of the straight line, respectively. A very high value of R^2 (0.99 > both for DW and HGW) suggested that this model is best suited for sorption data.

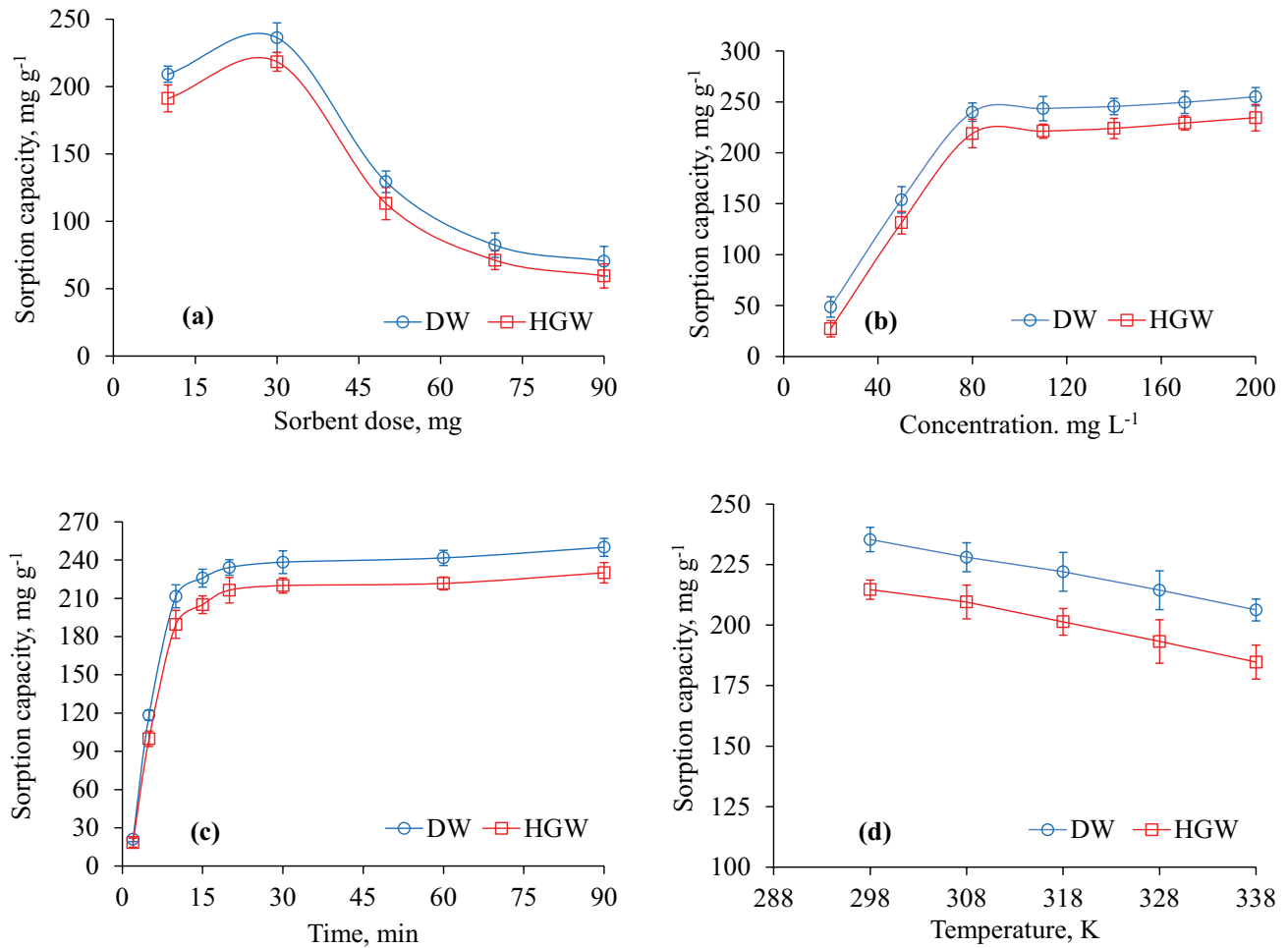


Fig. 7. Effect of sorbent dosage (10–90 mg) (a), initial metal ion concentration (20–200 mg L^{-1}) (b), contact time (2–90 min) (c), and temperature (298–338 K) (d), on sorption capacity (q_e in mg g^{-1}) of SSAVH for the removal of Cd^{2+} from DW and HGW (optimum sorption conditions: sorbent dose = 30 mg, $\text{pH} = 6$, Cd^{2+} concentration = 80 mg L^{-1} , contact time = 20 min, and temperature = 298 K in 100 mL solution for both DW and HGW).

Maximum sorption capacity (Q_{max}) 263.15 mg g^{-1} for DW and 243.90 mg g^{-1} for HGW were obtained. These high values of Q_{max} were also supported by the fact that sorbent contained a large concentration of sodium succinyl moieties as was evidenced by high DS value (Fig. 8b, Table 1). The validity of this model also gave evidence of the involvement of chemisorption by forming a monolayer. Moreover, some essential features of this model can be explained by calculating the values of a dimensionless constant, that is, R_L (separation factor) both for DW and HGW using Eq. (11):

$$R_L = \frac{1}{1 + bC_i} \quad (11)$$

In this Eq. (11), C_i (mg L^{-1}) is the initial concentration of metal ions and b (mg L^{-1}) is the Langmuir constant. The value of R_L is an indicator to decide the nature of the sorption process. In the case of zero value of R_L , the sorption process is reversible. The sorption process will be favorable and promising if R_L lies between 0 and 1 and unfavorable if greater than 1. The value of R_L was found between 0 and 1 for the

case under study (0.106 for DW and 0.126 for HGW), so, the sorption process was favorable.

To calculate the mean value of sorption energy and to investigate the nature of the sorption process either physical or chemical, experimental data were also fitted to the D–R model. A linear form of this isotherm is given in Eqs. (12–14):

$$\ln q_e = \ln X_m - \beta \varepsilon^2 \quad (12)$$

$$\varepsilon^2 = RT \ln \left(1 + \frac{1}{C_e} \right) \quad (13)$$

$$E = \frac{1}{\sqrt{-2\beta}} \quad (14)$$

where q_e (mg g^{-1}) is the amount of cadmium sorbed by SSAVH, C_e (mg L^{-1}) is the remaining concentration of cadmium at equilibrium, R is the ideal gas constant and

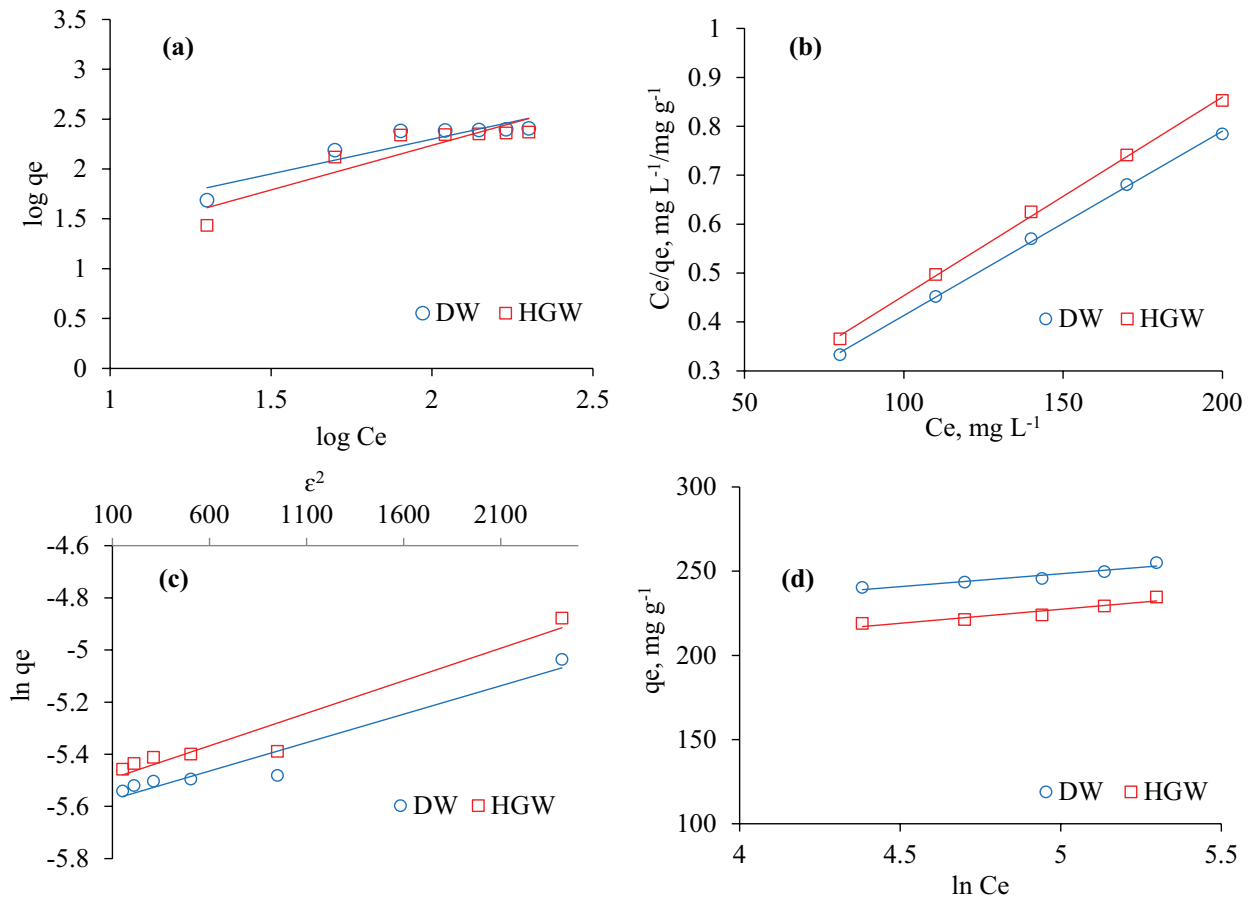


Fig. 8. Fitting of Freundlich sorption isotherm (a), Langmuir sorption isotherm (b), D–R isotherm (c), and Temkin isotherm (d) models for the removal of Cd^{2+} from DW and HGW solution using SSAVH (optimum sorption conditions: sorbent dose = 30 mg, pH = 6, Cd^{2+} concentration = 80 mg L^{-1} , contact time = 20 min, and temperature = 298 K in 100 mL solution for both DW and HGW).

T (K) shows absolute temperature, whereas, β ($\text{kJ}^2 \text{mol}^{-2}$), X_m (mg g^{-1}), and ε^2 are the constants associated with this model. Plotting of a graph between $\ln q_e$ against ε^2 (Fig. 8c, Table 1) gave straight lines and the values of constants were obtained from these straight lines. A high value of the regression coefficient was obtained which shows the validity of this model. The value of β in $\text{kJ}^2 \text{mol}^{-2}$ was used to calculate the value of E (mean sorption energy) in kJ mol^{-1} and it was found to be 11.96 kJ mol^{-1} for both DW and HGW. This value indicates that the sorption process occurs through chemisorption and particle diffusion [28].

Temkin isotherm model presumes that with the increase in surface exposure, the sorbate–sorbate interactions will also increase. Hence, the sorption heat of all the molecules in the layer will decrease and the whole sorption process is characterized by a uniform distribution of binding energies. The linear form of this isotherm can be depicted by Eq. (15):

$$q_e = B \ln A + B \ln C_e \quad (15)$$

where B is the ratio between the product of ideal gas constant (R) and absolute temperature T (K) to the constant related to sorption heat (b_s) and A (L min^{-1}) is the equilibrium

binding constant which corresponding to the maximum binding energy. The plot between q_e vs. $\ln C_e$ resulted in straight lines with a high value of R^2 . Slope ($B = RT/b_s$) and intercept ($B \ln A$) of the straight line were used to calculate the values of associated parameters (Fig. 8d, Table 1).

3.3.7. Kinetic modeling

The evaluation of sorption kinetics of the system is one of the important tools which describe the rate at which sorbent removes metal ions. Sorption kinetics also provides the effectiveness of the sorption mechanism by disclosing the mechanism of bonding and also directs toward valuable insight into the reaction pathways. So, for the analysis of sorption kinetics and to establish the sorption mechanism of Cd^{2+} removal, the experimental data obtained from contact time experiments were subjected to pseudo-first-order, pseudo-second-order, intraparticle diffusion, and Elovich models. Linear forms of the pseudo-first-order kinetic model and pseudo-second-order kinetic model are given by Eqs. (16) and (17):

$$\log(q_e - q_t) = \log q_e - \frac{k_1}{2.303} t \quad (16)$$

Table 1
Langmuir, Freundlich, D–R, Temkin, pseudo-second-order, pseudo-first-order, intraparticle diffusion, Elovich, ion exchange models, and thermodynamic parameters for the removal of Cd²⁺ from DW and HGW solution using SSAVH

Models	Parameters	DW	HGW
Experimental parameters	q_e (mg g ⁻¹)	240.26	218.93
	Q_{\max} (mg g ⁻¹)	263.15	243.90
	Q_{\max} (mmol g ⁻¹)	2.35	2.18
	b (mg L ⁻¹)	0.105	0.0863
	R^2	0.9991	0.9987
Freundlich parameters	R_L	0.106	0.126
	n	1.434	1.117
	K_F	8.043	2.794
D–R constants	R^2	0.8449	0.8295
	β (kJ ² mol ⁻²)	-0.0002	-0.0002
	X_m (mmol g ⁻¹)	0.00372	0.00402
	R^2	0.9376	0.938
Temkin constants	E (kcal mol ⁻¹)	11.96	11.96
	B	15.214	16.5921
	A	8E ⁴	6E ³
	b_T	162.85	152.07
Pseudo-second-order	R^2	0.9199	0.9039
	q_e (mg g ⁻¹)	256.41	232.55
	k_2 (g mg ⁻¹ min ⁻¹)	0.00195	0.0022
Pseudo-first-order	R^2	0.9996	0.9993
	q_e (mg g ⁻¹)	93.46	89.41
	k_1 (g mg ⁻¹ min ⁻¹)	0.0511	0.0514
Interparticle diffusion	R^2	0.6638	0.6525
	k_{idm} (mg g ⁻¹ min ^{1/2})	3.0344	3.001
	C	215.22	196.08
Elovich model	R^2	0.954	0.9026
	α (mg (g min) ⁻¹)	3E ⁸	8E ⁷
	β (g mg ⁻¹)	0.08703	0.08958
Ion exchange model	R^2	0.9231	0.8413
	S (min ⁻¹)	0.152	0.1384
	R^2	0.9501	0.963
Thermodynamics	ΔS° (J mol ⁻¹ K ⁻¹)	-27.84	-21.1253
	ΔH° (kJ mol ⁻¹)	-16.251	-12.889
	ΔG° (kJ mol ⁻¹)	-7.98	-6.496
	R^2	0.9985	0.9933

$$\frac{t}{q_t} = \frac{1}{q_e^2 k_2} + \frac{t}{q_e} \quad (17)$$

where q_e (mg g⁻¹) and q_t (mg g⁻¹) are the amounts of Cd²⁺ adsorbed at equilibrium and at time t , respectively while k_1 (g mg⁻¹ min⁻¹) and k_2 (g mg⁻¹ min⁻¹) are the constants associated with these models and representing rate constant for pseudo-first-order and pseudo-second-order reactions, respectively. Plotting of graph between $\log(q_e - q_t)$ vs. t for pseudo-first-order reaction and t/q_t vs. t/q_e for pseudo-second-order reaction gave straight lines. From the slopes and intercepts of these straight lines, the values of constants

associated with these models were calculated for both DW and HGW (Figs. 9a and b, Table 1). Very low values of R^2 suggested that the experimental data did not fit the pseudo-first-order kinetic model while a high value of R^2 (>0.99) for both DW and HGW suggested the better fit of pseudo-second-order kinetic model to experimental data. Fitting of the pseudo-second-order kinetic model showed the involvement of the chemisorption mechanism in the rate-determining step.

The intraparticle diffusion kinetic model is considered to be a very useful tool for establishing the rate-determining step (slowest step) in any solid–liquid sorption system having porous sorbents. According to this model, the amount of metal adsorbed (q_e in mg g⁻¹) varies directly with the square root of time (t in min) as presented in Eq. (18):

$$q_t = k_{\text{idm}} t^{1/2} + C \quad (18)$$

where k_{idm} (mg g⁻¹ min^{1/2}) is intraparticle diffusion rate constant and C is the intercept. The values of these constants were determined from the slope and intercept of a straight line obtained by plotting the graph between q_t and $t^{1/2}$ (Fig. 9c). The validity of this model can be judged through the behavior of a straight line. If the straight-line passes through the origin, then intraparticle diffusion is simply considered to be the rate-determining step. Whereas, if a straight line does not pass through the origin then both chemisorption and intraparticle diffusion contribute to the rate-determining step. In the case under study, the straight lines do not pass through the origin, so sorption of Cd²⁺ from DW and HGW occur through chemisorption mechanism and intraparticle diffusion.

To confirm the mechanism of the sorption process for the removal of Cd²⁺ from DW and HGW, the use of the Elovich equation is also fruitful. The linear form of this equation is presented in Eq. (19):

$$q_t = \frac{1}{\beta} \ln(\alpha\beta) + \frac{1}{\beta} \ln t \quad (19)$$

where q_t is the amount of Cd²⁺ ion removed at time t in mg g⁻¹, β (g mg⁻¹) and α (mg (g min)⁻¹) are the Elovich constants representing the energy of activation of chemisorption and rate of chemical sorption at zero coverage. The plot of the graph between $\ln t$ vs. q_e gives straight lines with a high value of correlation coefficient which might suggest the involvement of chemisorption sharing or exchange of electrons between sorbent and sorbate. Slope and intercepts of the straight lines were utilized to obtain the values of associated parameters (Fig. 9d, Table 1).

3.3.8. Sorption mechanism

The SAVH (acidic form) showed insignificant sorption (12% from DW and 9.5% from HGW), whereas, SSAVH (sodic form) showed significantly high metal uptake (93.5% from DW and 92% from HGW). These high values of sorption by SSAVH might be attributed to the exchange of Cd²⁺ ions in solution and Na⁺ ions present in the sodic form of the sorbent (SSAVH) (Fig. 12c). So, the ion exchange or chemisorption process was thought to be responsible for

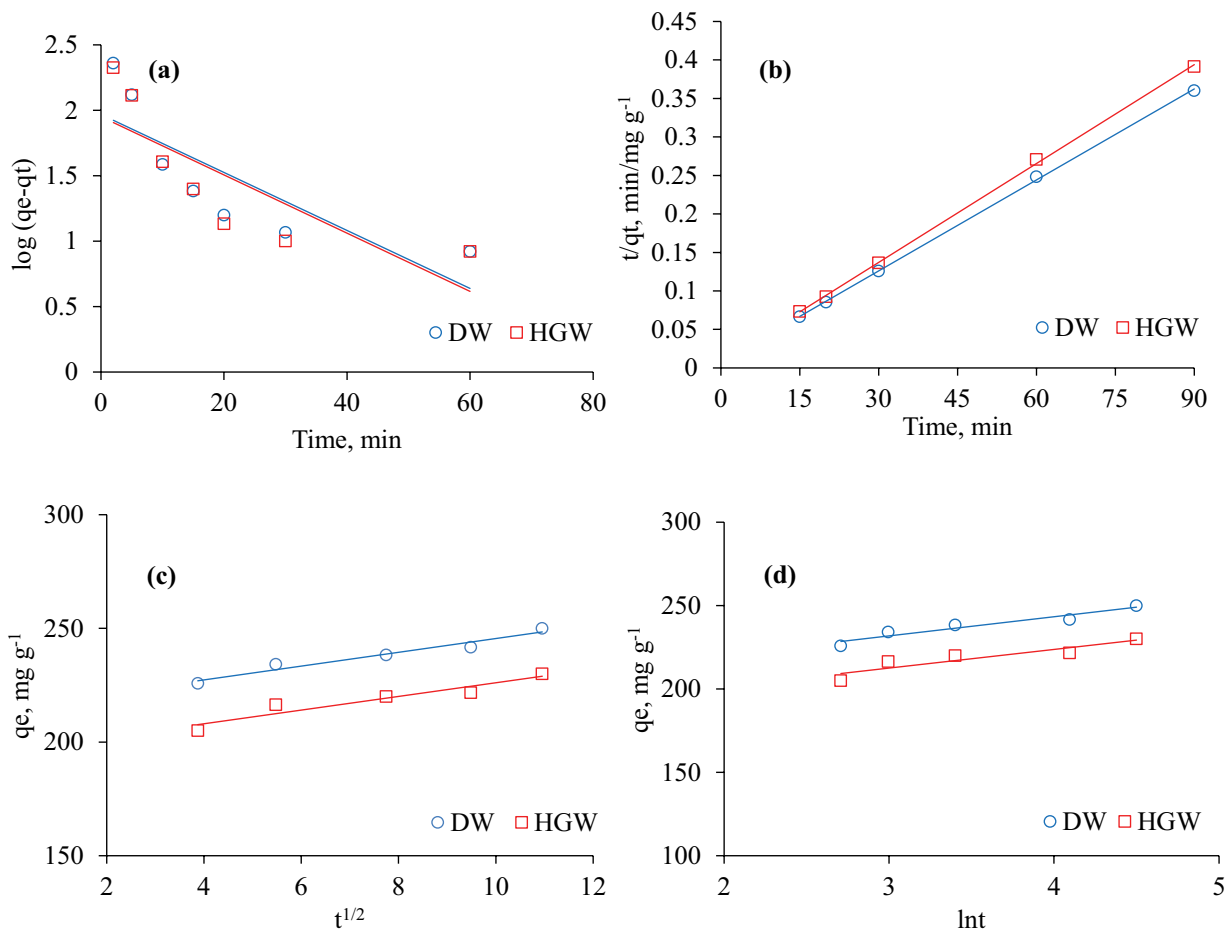


Fig. 9. Fitting of pseudo-first-order (a), pseudo-second-order (b), intraparticle diffusion (c), and Elovich (d) kinetic models for the removal of Cd²⁺ from DW and HGW solution using SSAVH (optimum sorption conditions: sorbent dose = 30 mg, pH = 6, Cd²⁺ concentration = 80 mg L⁻¹, contact time = 20 min, and temperature = 298 K in 100 mL solution for both DW and HGW).

metal ions removal from DW and HGW. The establishment of this mechanism was also supported by the successful fitting of the Langmuir isotherm model, pseudo-second-order kinetic model, D-R model, Tempkin model, and Elovich model to the experimental data. Boyd et al. [29] rate equation (Eq. (20)) was used to describe the rate at which the exchange of ions would take place.

$$\log(1 - F) = -\frac{S}{2.303} t \tag{20}$$

where F is the ratio between amounts of metal sorbed at equilibrium (q_e) and amounts of metal sorbed at time t (q_t) and S (min⁻¹) is sorption constant. The involvement of the ion exchange mechanism can be predicted by plotting the graph between $\log(1 - F)$ against t . A high value of the correlation coefficient as abstracted from the straight line is evident for the fitting of this ion-exchange model (Fig. 10, Table 1).

3.3.9. Determination of thermodynamic parameters

The data obtained from the effect of temperature experiments on Cd²⁺ sorption was used to determine the values

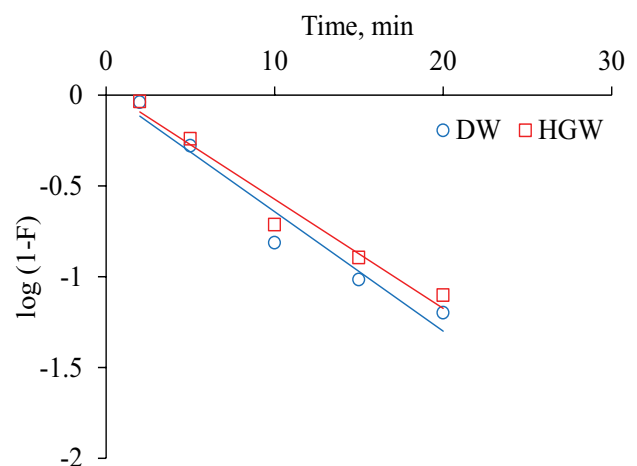


Fig. 10. Ion-exchange model for the sorption of Cd²⁺ by SSAVH (optimum sorption conditions: sorbent dose = 30 mg, pH = 6, Cd²⁺ concentration = 80 mg L⁻¹, contact time = 20 min, and temperature = 298 K in 100 mL solution for both DW and HGW).

Table 2

Comparison of SSAVH sorption capacity with other polysaccharide-based modified reported sorbents for Cd²⁺ sorption

Sorbent used	Sorption capacities (Q_{\max} in mg g ⁻¹)	References
Maize straw, chemically modified with succinic anhydride	196.1	[30]
Sugarcane bagasse, chemically modified with succinic anhydride	196	[31]
Cellulose, chemically modified with succinic anhydride, sodic	185.2 from DW 178.6 from GW	[32]
Glucuronoxylan, chemically modified with succinic anhydride, sodic	144.9 from DW 138.9 from GW	[19]
Sawdust, chemically modified with polyacrylic acid	76.1 and 168	[33]
Mercerized cellulose, chemically modified with succinic anhydride	88	[34]
Mercerized sugarcane bagasse, chemically modified with ethylenetetramine	86.2 and 106.4	[35]
Welan gum chemically modified cellulose beads, modified with succinic anhydride	83.6	[36]
AVH, chemically modified with succinic anhydride, sodic	263.15 from DW 243.90 from HGW	Present study

The values of sorption capacities (Q_{\max} in mg g⁻¹) of all the sorbent coated in Table 2 are calculated by Langmuir isothermal model.

of the thermodynamic triplet (ΔG° , ΔS° , and ΔH°). A graph was plotted between $\ln K_c$ and $1/T$ (K⁻¹). straight-line was obtained. Slope and intercept of this straight line were used to find the values of ΔG° and ΔH° , respectively (Eq. (7), Fig. 11). These values were put into Vant's Hoff equation (Eq. (8)) to calculate the value of ΔS° . These values are presented in Table 1. Negative values of ΔG° and ΔH° suggest the feasibility, spontaneity, and exothermic nature of sorption process while the negative value of ΔS° indicates the existence of strong intermolecular forces between sorbent (SSAVH) and sorbate (Cd²⁺ ion solution) and deterioration in the randomness of sorbent to adsorb metal ions.

The comparison of position of the present sorbent with other already known sorbents of similar nature (i.e., succinylated polysaccharide materials) shows that present sorbent has a prominent position among the other polysaccharidal sorbents (i.e., succinylated cellulosic materials) for Cd-uptake as can be evidenced from Table 2.

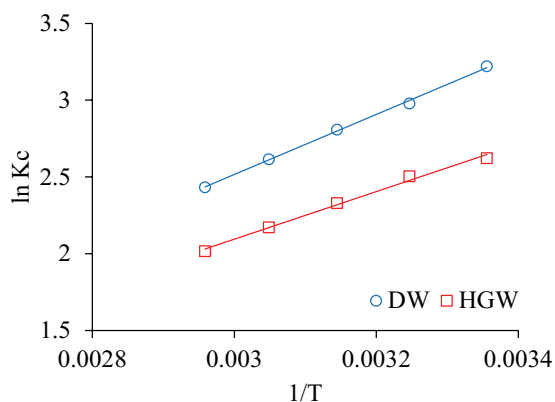


Fig. 11. Effect of temperature on equilibrium constant for the sorption of Cd²⁺ by SSAVH (optimum sorption conditions: sorbent dose = 30 mg, pH = 6, Cd²⁺ concentration = 80 mg L⁻¹, contact time = 20 min, and temperature = 298 K in 100 mL solution for both DW and HGW).

3.3.10. Sorption–desorption studies

The effectiveness of any sorbent toward its metal uptake capability can be judged through regeneration studies. By maintaining optimal conditions, sorption–desorption studies were carried out over five consecutive cycles. Figs. 12a and b show that a sorption capacity decrease of 18.7 and 17.9 mg g⁻¹ were observed for DW and HGW after five cycles. Likewise, Fig. 12c represents Cd²⁺ uptake by SSAV over five cycles in terms of percentage metal-uptake. From the results, it was inferred that a 2.9% sorption capacity decrease was observed in the case of DW, whereas, a 4.1% decrease in the case of HGW. These results suggested that SSAVH can be used repeatedly before we need to replace it.

4. Conclusion

The sodium salt of AVH was evaluated for its effectiveness for the remove Cd²⁺ from DW and HGW and it appeared as a supersorbent as evident from its high sorption capacity. The sorption data revealed that the sorbent under discussion appeared highly efficient and selective for Cd²⁺ uptake. Sorption process followed the ion-exchange mechanism and efficiently removed 90% of Cd²⁺ in first 20 min. The sorbent appeared re-generable over five cycles with insignificant decrease in sorption capacity which make it a potential candidate for industrial applications. Concluding, SSAVH is a very efficient and reusable supersorbent for Cd²⁺ uptake from DW and HGW that should be further exploited for other toxic metal ion uptake for real-world solutions.

Acknowledgments

We are grateful to ORIC University of Sargodha Pakistan for the financial support under grant number UOS/ORIC/2016/52. HA acknowledges Nick Rees, Oxford University, for collecting some of the NMR data.

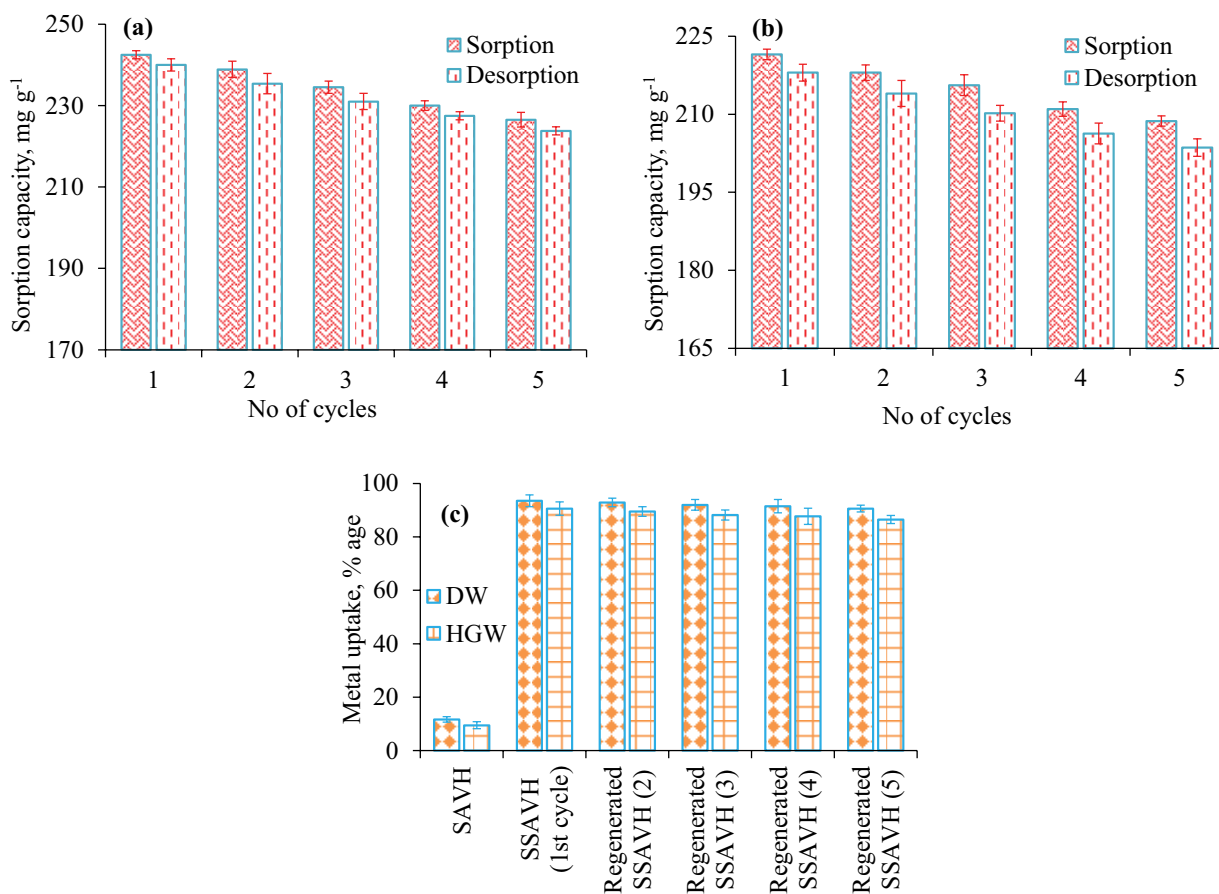


Fig. 12. Sorption and desorption of Cd²⁺ from (a) DW, (b) HGW, and (c) Percentage Cd²⁺ uptake, by SAVH and SSAVH (sorption conditions: sorbent dose = 30 mg, pH = 6, Cd²⁺ concentration = 80 mg L⁻¹, contact time = 20 min, and temperature = 298 K in 100 mL solution for both DW and HGW; desorption conditions: sorbent dose = 30 mg, pH = 6, Cd²⁺ concentration = 80 mg L⁻¹, contact time = 24 h, and temperature = 298 K 100 mL of saturated solution of 1 M NaCl).

We are grateful to Mr. Sarfraz Ahmad, Pakistan Council of Research in Water Resource (PCRWR), Sargodha, Pakistan for helpful discussion and provision of the HGW samples analyses.

References

- [1] H. Ali, E. Khan, I. Ilahi, Environmental chemistry and ecotoxicology of hazardous heavy metals: Environmental persistence, toxicity and bioaccumulation, *J. Chem.*, 2019 (2019) 6730305, doi: 10.1155/2019/6730305.
- [2] J.L. Ovesen, Y. Fan, J. Chen, M. Medvedovic, Y. Xia, A. Puga, Long-term exposure to low-concentrations of Cr(VI) induce DNA damage and disrupt the transcriptional response to benzo[a]pyrene, *Toxicology*, 316 (2014) 14–24.
- [3] D.A. Halwani, M. Jurdi, F.K.A. Salem, M.A. Jafa, N. Amacha, R.R. Habib, H.R. Dhaini, Cadmium health risk assessment and anthropogenic sources of pollution in Mount-Lebanon Springs, *Exposure Health*, 12 (2020) 163–178.
- [4] L. Torres-Sanchez, R.A. Vazquez-Salas, A. Vite, M. Galvan-Portillo, M.E. Cebrian, A.P. Macias-Jimenez, C. Rios, S. Montes, Blood cadmium determinants among males over forty living in Mexico City, *Sci. Total Environ.*, 637–638 (2018) 686–694.
- [5] H. Wu, Q. Liao, S.N. Chillrud, Q. Yang, L. Huang, J. Bi, B. Yan, Environmental exposure to cadmium: Health risk assessment and its associations with hypertension and impaired kidney function, *Sci. Rep.*, 6 (2016) 29989, doi: 10.1038/srep29989.
- [6] A. Bernard, Cadmium and its adverse effects on humans, *Indian J. Med. Res.*, 128 (2008) 557–564.
- [7] L. Cai, J. Sun, L. Cui, Y. Jiang, Z. Huang, Stabilization of heavy metals in piggery wastewater sludge through coagulation-hydrothermal reaction-pyrolysis process and sludge biochar for tylosin removal, *J. Cleaner Prod.*, 260 (2020) 121165, doi: 10.1016/j.jclepro.2020.121165.
- [8] Z.A. Alothman, Y.E. Unsal, M. Habila, M. Tuzen, M. Soylak, A membrane filtration procedure for the enrichment, separation, and flame atomic absorption spectrometric determinations of some metals in water, hair, urine, and fish samples, *Desal. Water Treat.*, 53 (2015) 3457–3465.
- [9] J.Q. Tang, J.B. Xi, J.X. Yu, R.A. Chi, J.D. Chen, Novel combined method of biosorption and chemical precipitation for recovery of Pb²⁺ from wastewater, *Environ. Sci. Pollut. Res.*, 25 (2018) 28705–28712.
- [10] P. Halli, V. Agarwal, J. Partinen, M. Lundsrom, Recovery of Pb and Zn from a citrate leach liquor of a roasted EAF dust using precipitation and solvent extraction, *Sep. Purif. Technol.*, 236 (2020), 116264 doi: 10.1016/j.seppur.2019.116264.
- [11] J. Kheriji, D. Tabassi, B. Hamrouni, Removal of Cd(II) ions from aqueous solution and industrial effluent using reverse osmosis and nanofiltration membranes, *Water Sci. Technol.*, 72 (2015) 1206–1216.
- [12] L.A. Malik, A. Bashir, T. Manzoor, A.H. Pandith, Microwave assisted synthesis of glutathione coated hallow zinc oxide for the removal of heavy metal ions from aqueous system, *RSC Adv.*, 9 (2019) 15976–15985.

- [13] W. He, K. Ai, X. Ren, S. Wang, L. Lu, Inorganic layered ion exchangers for decontamination of toxic metal ions in aquatic systems, *J. Mater. Chem. A*, 5 (2017) 19593–19606.
- [14] S. He, Y. Li, L. Weng, J. Wang, J. He, Y. Liu, K. Zhang, Q. Wu, Y. Zhang, Z. Zhang, Competitive adsorption of Cd^{2+} , Pb^{2+} and Ni^{2+} onto Fe^{3+} modified argillaceous limestone: Influence of pH, ionic strength and natural organic matters, *Sci. Total Environ.*, 637–638 (2018) 69–78.
- [15] W.S.W. Ngah, S. Fatinathan, Pb(II) biosorption using chitosan and chitosan derivatives beads: equilibrium, ion exchange and mechanism studies, *J. Environ. Sci.*, 22 (2010) 338–346.
- [16] K.S. Rao, M. Mohapatra, S. Anand, P. Venkateswarlu, Review on cadmium removal from aqueous solutions, *Int. J. Eng. Sci. Technol.*, 2 (2010) 81–103.
- [17] A. Abbas, M.A. Hussain, M. Sher, M.I. Irfan, M.N. Tahir, W. Tremel, S.Z. Hussain, I. Hussain, Design, characterization and evaluation of hydroxyl ethyl cellulose based novel regenerable super-sorbent for heavy metal ions uptake and competitive adsorption, *Int. J. Biol. Macromol.*, 102 (2017) 170–180.
- [18] A. Abbas, M.A. Hussain, M. Sher, N.S. Abbas, M. Ali, Modified hydroxyethylcellulose: a regenerable supersorbent for Cd^{2+} uptake from spiked high-hardness groundwater, *Cellulose Chem. Technol.*, 51 (2017) 167–174.
- [19] G. Muhammad, A. Abbas, M.A. Hussain, M. Sher, S.N. Abbas, Chemically modified glucuronoxylan: a novel material for heavy metal ion removal from aqueous and spiked high hardness groundwater, *Cellulose Chem. Technol.*, 52 (2018) 909–919.
- [20] B.A. Lodhi, A. Abbas, M.A. Hussain, S.Z. Hussain, M. Sher, I. Hussain, Design, characterization and appraisal of chemically modified polysaccharide based mucilage from *Ocimum basilicum* (basil) seeds for the removal of $\text{Cd}(\text{II})$ from spiked high-hardness ground water, *J. Mol. Liq.*, 274 (2019) 15–24.
- [21] M. Farid-ul-Haq, M.A. Hussain, M.T. Haseeb, M.U. Ashraf, S.Z. Hussain, T. Tabassum, I. Hussain, M. Sher, S.N.A. Bukhari, M. Naeem-ul-Hassan, A stimuli-responsive, superporous and non-toxic smart hydrogel from seeds of mugwort (*Artemisia vulgaris*): stimuli responsive swelling/deswelling, intelligent drug delivery and enhanced aceclofenac bioavailability, *RSC Adv.*, 10 (2020) 19832–19843, doi: 10.1039/d0ra03176c.
- [22] A. Abbas, M.A. Hussain, M. Amin, M. Sher, M.N. Tahir, W. Tremel, Succinate-bonded pullulan: an efficient and reusable super-sorbent for cadmium-uptake from spiked high-hardness groundwater, *J. Environ. Sci.*, 37 (2015) 51–58.
- [23] V. Aghazadeh, S. Barakan, E. Bidari, Determination of surface protonation deprotonation behavior, surface charge, and total surface site concentration for natural, pillared and porous nano bentonite heterostructure, *J. Mol. Struct.*, 1204 (2020) 127570, doi: 10.1016/j.molstruc.2019.127570.
- [24] S. Fan, J. Zhou, Y. Zhang, Z. Feng, H. Hu, Z. Huang, Y. Qin, Preparation of sugarcane bagasse succinate/alginate porous gel beads via a self-assembly strategy: improving the structural stability and adsorption efficiency for heavy metal ions, *Bioresour. Technol.*, 306 (2020) 123–128.
- [25] Y. Yang, Y. Chun, G. Sheng, M. Huang, pH-dependence of pesticides adsorption by wheat-residue-derived black carbon, *Langmuir*, 20 (2004) 6736–6741.
- [26] A. Abbas, M.A. Hussain, M. Sher, S.Z. Hussain, I. Hussain, Evaluation of chemically modified polysaccharide pullulan as an efficient and regenerable supersorbent for heavy metal ions uptake from single and multiple metal ion systems, *Desal. Water Treat.*, 78 (2017) 241–252.
- [27] H. Shehzad, E. Ahmed, A. Sharif, M.I. Din, Z.H. Farooqi, I. Nawaz, R. Bano, M. Iftikhar, Amino-carbamate moiety grafted calcium alginate hydrogel beads for effective biosorption of $\text{Ag}(\text{I})$ from aqueous solution: economically-competitive recovery, *Int. J. Biol. Macromol.*, 144 (2020) 362–372.
- [28] R.S. Juang, M.L. Chen, Application of the Elovich equation to the kinetics of metal sorption with solvent-impregnated resins, *Ind. Eng. Chem. Res.*, 36 (1997) 813–820.
- [29] G.E. Boyd, A.W. Adamson, L.S. Myers, The exchange adsorption of ions from aqueous solutions by organic zeolites. II. Kinetics, *J. Am. Chem. Soc.*, 69 (1947) 2836–2848.
- [30] H. Guo, S. Zhang, Z. Kou, S. Zhai, W. Ma, Y. Yang, Removal of cadmium(II) from aqueous solutions by chemically modified maize straw, *Carbohydr. Polym.*, 115 (2015) 177–85.
- [31] O. Karnitz Jr., L.V.A. Gurgel, J.C.P. de Melo, V.R. Botaro, T.M.S. Melo, R.P. de Freitas Gil, L.F. Gil, Adsorption of heavy metal ion from aqueous single metal solution by chemically modified sugarcane bagasse, *Bioresour. Technol.*, 98 (2007) 1291–1297.
- [32] B. Belhallaoui, A. Aziz, E.H. Elandaloussi, M.S. Ouali, L.C. De Menorval, Succinate-bonded cellulose: a regenerable and powerful sorbent for cadmium-removal from spiked high-hardness groundwater, *J. Hazard. Mater.*, 169 (2009) 831–837.
- [33] M. Geay, V. Marchetti, A. Clement, B. Loubinoux, P. Gerardin, Decontamination of synthetic solutions containing heavy metals using chemically modified sawdusts bearing polyacrylic acid chains, *J. Wood Sci.*, 46 (2000) 331–333.
- [34] L.V.A. Gurgel, O.K. Junior, R.P.F. Gil, L.F. Gil, Adsorption of $\text{Cu}(\text{II})$, $\text{Cd}(\text{II})$ and $\text{Pb}(\text{II})$ from aqueous single metal solutions by cellulose and mercerized cellulose chemically modified with succinic anhydride, *Bioresour. Technol.*, 99 (2008) 3077–3083.
- [35] L.V.A. Gurgel, L.F. Gil, Adsorption of $\text{Cu}(\text{II})$, $\text{Cd}(\text{II})$ and $\text{Pb}(\text{II})$ from aqueous single metal solutions by succinylated twice-mercerized sugarcane bagasse functionalized with triethylenetetramine, *Water Res.*, 43 (2009) 4479–4488.
- [36] J. Liu, T.H. Xie, C. Deng, K.F. Du, N. Zhang, J.J. Yu, Y.L. Zou, Y.K. Zhang, Welan gum-modified cellulose bead as an effective adsorbent of heavy metal ions (Pb^{2+} , Cu^{2+} , and Cd^{2+}) in aqueous solution, *Sep. Sci. Technol.*, 49 (2014) 1096–1103.